

Scattering of a plane wave by a perfectly conducting cylinder

N. Heidari¹*, Caio F. B. Macedo^{2†}, A. A. Araújo Filho^{3‡} and H. Hassanabadi^{1,4§}

¹Faculty of Physics, Shahrood University of Technology, Shahrood, Iran.

²Faculdade de Física, Campus Salinópolis, Universidade Federal do Pará, 68721 – 000, Salinópolis, Pará, Brazil.

³Departamento de Física, Universidade Federal da Paraíba, Caixa Postal 5008, 58051–970, João Pessoa, Paraíba, Brazil.

⁴Department of Physics, University of Hradec Králové, Rokytanského 62, 500 03 Hradec Králové, Czechia.

Abstract

In this work, we study the scattering of a plane wave by a perfectly conducting cylinder. The problem is solved using the method of separation of variables. The exact solution is obtained in terms of Bessel and Hankel functions. The asymptotic behavior of the scattered wave is analyzed in the far field. The results show that the scattering cross-section is independent of the frequency of the incident wave. The numerical results are compared with the analytical ones. The results show that the scattering cross-section is independent of the frequency of the incident wave.

Keywords: Scattering; Perfectly Conducting Cylinder; Asymptotic Behavior.

1 Introduction

Longitudinal waves in a perfectly conducting cylinder are of great interest in many applications. The problem of scattering of a plane wave by a perfectly conducting cylinder is a classical problem in physics. The exact solution is obtained in terms of Bessel and Hankel functions. The asymptotic behavior of the scattered wave is analyzed in the far field. The results show that the scattering cross-section is independent of the frequency of the incident wave.

Recently, there has been a growing interest in the study of scattering of longitudinal waves by a perfectly conducting cylinder. The problem is solved using the method of separation of variables. The exact solution is obtained in terms of Bessel and Hankel functions. The asymptotic behavior of the scattered wave is analyzed in the far field. The results show that the scattering cross-section is independent of the frequency of the incident wave.

*E-mail: heidari@shmtu.ac.ir

†E-mail: caio@fisica.ufpa.br

‡E-mail: araujo@fisica.ufpb.br

§E-mail: hassanabadi@shmtu.ac.ir

despate na apLorinne in nliged ghe
es[1246], p[17, 18], onr pcebs[19, 20], balgv
ides[21, 22], pcebmies[23, 24], ad (ch) field h[25, 26]
h[2528], ad Ho na-L[29] ad ch[30, 31].

Ehmadath c[6]L[7]beah(LSB) des
abb h[8] chacesh[9] U[10]. The p[11] based ch
beath d[12]ag, h[13] ch U[14] n[15]sh chaces[16] sa[17]
L[18][32]. Th[19] h[20] p[21] ched t[22]LSB ash[23]
p[24] i[25][33]. S[26]e h[27] n[28]sh[29] ex[30] ad[31] n[32] h[33]
g[34], P[35]ad M[36] p[37]ections[35, 36], CPT[38]ad CPT[39]d LV
e[40][3740], h[41]rd[42]p[43][41, 42], b[44]e[45] des[43],
i[44], ad E[45]h[46]h[47][45]. The d[48]e[49]c[50]t[51]e[52]h[53]e[54] m[55]e[56]d[57]
h[58]p[59]LSB i[60]n[61]c[62]al[63]f[64]i[65]e[66]d[67] M[68]o[69]r[70] h[71]g[72]L[73]
p[74]e[75]a[76]h[77]f[78]i[79]e[80]p[81]i[82]q[83] ch[84]g[85]s[86]d[87]at[88]f[89]
n[90]L[91]o[92]h[93](LV) e[94]x[95]i[96]g[97]i[98]n[99]l[100]f[101]i[102]e[103]d[104] h[105]os[106] In[107]fl[108]at[109]p[110]ce[111]bs[112] ad-
d[113]e[114] LV e[115]n[116]sh[117] C[118]a[119]r[120]d[121]Jack[122][46] ad a[123]e[124]b[125]r[126]e[127][47, 48], car[128]be[129] d[130]ued
s[131]a[132]b[133]y[134] F[135]ra[136] c[137]p[138]a[139]p[140]h[141]e[142]n[143]g[144]al[145]p[146]e[147] LV i[148]n[149]c[150]p[151]e[152]r[153]
t[154][49].

rainbow gv

Th[505] Sad[506]ad M[507]de[508]E[509]i[510](SME), e[511]n[512]g[513]i[514]n[515]e[516]c[517]p[518]a[519]s[520]a[521] co[522]e
ad i[523]n[524] f[525]i[526]e[527]l[528]d[529] p[530]h[531]y[532] ad[533]d[534]r[535]e[536]s[537]al[538]p[539]h[540] co[541]f[542]i[543]c[544]e[545]t[546]s[547]L[548]o[549]r[550]
h[551][5057]. Sp[552]e[553]c[554]i[555]f[556]i[557]c[558]ally[559] h[560]i[561]g[562]h[563] SME p[564]a[565]r[566]a[567] R[568]e[569]n[570]e[571]
a[572]n[573]d, d[574]i[575]a[576]l[577]c[578]e[579]g[580]i[581]a[582] g[583]o[584]t[585] q[586]u[587]a[588]l[589]e[590] h[591] e[592]t[593]. A[594]
h[595]e[596] i[597]n[598]t[599]r[600]o[601]d[602]u[603]e[604] R[605]e[606]n[607]e[608]s[609]i[610]n[611]g[612]i[613] SME s[614]c[615]e[616]n[617]a[618]r[619]e[620]
p[621]o[622]l[623]i[624]t[625]i[626]c[627] h[628] e[629]t[630] a[631]p[632]p[633]h[634]e[635] h[636] e[637]t[638] s[639]a[640]s[641]h[642] h[643]
d[644]i[645]a[646]l[647]e[648]t[649] f[650]i[651]e[652].

I[653]n[654]c[655]o[656]r[657]p[658]o[659]s[660]e[661]d[662] h[663]o[664]d[665] n[666]e[667]g[668]a[669]t[670]i[671]o[672]n[673]
i[674]n[675]p[676]e[677] L[678]o[679]r[680]y[681]beah(LSB) i[682]n[683]d[684] p[685]ce[686]bs[687] N[688]o[689]b[690]e[691] ex[692]p[693]
d[694]e[695]s[696]c[697]r[698]i[699]b[700]e[701]e[702] g[703]i[704]g[705]h[706] e[707]t[708] a[709]p[710]h[711][5868], h[712] E[713]h[714]e[715]r[716]d[717]e[718]
l[719][69], p[720]h[721]e[722]s[723][7075], ad C[724]h[725]i[726]s[727]t[728]i[729]f[730]i[731]e[732]d[733] g[734][7678]. E[735]x[736]a[737]
m[738]p[739]l[740]e[741]s[742] h[743]e[744] a[745]b[746]e[747]e[748]r[749]e[750]d[751]u[752]e[753]d[754] t[755]o[756] d[757]e[758]t[759]e[760]c[761]t[762]g[763]i[764]f[765]LSB i[766]n[767] e[768]a[769]k[770]
f[771]i[772]e[773]l[774]d[775] e[776]x[777]i[778]g[779]i[780]n[781]l[782]f[783]i[784]e[785]l[786]d[787]s[788] i[789]n[790]
S[791]h[792]r[793]S[794]e[795]m[796]p[797]t[798]i[799]c[800]h[801]e[802] [7981]. Th[803]e[804] e[805]c[806]t[807]e[808]c[809]t[810]
a[811]s[812]y[813]h[814] LIGO/VIRGO c[815]h[816]o[817]l[818]l[819] [82], e[820]n[821]b[822]e[823]d[824] b[825]y[826] a[827]n[828]
e[829]n[830]t[831]i[832]c[833]h[834]p[835]ad[836] a[837]n[838]t[839]i[840]g[841]h[842] f[843]i[844]e[845]l[846] e[847]n[848]g[849]i[850]n[851]
p[852]h[853] T[854]e[855]l[856]e[857]p[858]h[859]a[860] p[861]h[862]
t[863]h[864]e[865] p[866]e[867]s[868]p[869]e[870]c[871]t[872]i[873]c[874]s[875] s[876]h[877]a[878]s[879]b[880]a[881]c[882]
k[883]s[884] i[885]n[886] h[887]o[888]d[889]s[890]
h[891]e[892] a[893]b[894]a[895]d[896]y[897]b[898]e[899]e[900]r[901]p[902]i[903]n[904]g[905][83, 84].

Wh[906]e[907]n[908] m[909]u[910]l[911]t[912]i[913]p[914]l[915]y[916] d[917]i[918]e[919]d[920] h[921]o[922]s[923]t[924]i[925]g[926]h[927] a[928]d[929]d[930]i[931]
e[932]t[933] a[934]p[935]h[936] h[937]e[938] i[939]n[940]c[941]r[942]e[943]s[944]i[945]m[946]e[947]n[948]t[949]a[950]l[951] g[952]o[953]t[954] f[955]i[956]
e[957]l[958]d[959] N[960]o[961]b[962]y[963]e[964]a[965]t[966]h[967]i[968]s[969] f[970]r[971]
t[972]h[973]e[974] R[975]e[976]n[977]e[978]s[979]i[980]n[981]g[982]i[983] s[984]p[985]e[986]c[987]i[988]f[989]i[990]
c[991]a[992]n[993]b[994]a[995]c[996]k[997] s[998]p[999]e[1000]c[1001]i[1002]f[1003] a[1004]d[1005]a[1006]n[1007]g[1008]
s[1009]h[1010]a[1011]s[1012] h[1013] i[1014]d[1015]o[1016]t[1017]b[1018] g[1019]i[1020]n[1021]
p[1022]a[1023]l[1024]e[1025][85]. A[1026]b[1027]r[1028]i[1029]g[1030]o[1031]n[1032]g[1033] F[1034]r[1035]e[1036]
n[1037]g[1038]e[1039][86], h[1040]h[1041]a[1042]s[1043]b[1044]e[1045]e[1046]n[1047]e[1048]d[1049] L[1050]o[1051]r[1052]
y[1053]beah(LSB) i[1054]n[1055]v[1056]e[1057]s[1058]-
e[1059]s[1060][8791].

Th[1061]e[1062] r[1063]a[1064]f[1065]a[1066] (Pah) i[1067]n[1068]t[1069]e[1070]r[1071]n[1072]e[1073]s[1074] a[1075]b[1076]e[1077] g[1078]a[1079]n[1080]
k[1081]i[1082]t[1083]h[1084] e[1085]t[1086] a[1087]p[1088]l[1089]y[1090] e[1091]a[1092]c[1093]
h[1094] e[1095]t[1096] ad[1097] c[1098]o[1099]n[1100]s[1101]i[1102]d[1103]e[1104]p[1105]e[1106]n[1107]d[1108]
g[1109]a[1110]l[1111]p[1112]h[1113]e[1114] [92, 93]. D[1115]e[1116]p[1117] a[1118]d[1119]a[1120]
n[1121]t[1122]i[1123]c[1124]h[1125]L[1126]o[1127]n[1128] y[1129]beah[1130]e[1131]
n[1132]d[1133] e[1134]t[1135]h[1136]e[1137]p[1138]. H[1139]o[1140]w[1141]e[1142]r[1143], e[1144]c[1145]
e[1146]t[1147]h[1148]e[1149] b[1150]e[1151]g[1152]a[1153]d[1154]-
d[1155]e[1156]s[1157]p[1158]e[1159]c[1160]t[1161]i[1162]c[1163]h[1164] c[1165]o[1166]k[1167]b[1168]e[1169]
e[1170]g[1171]e[1172]n[1173]s[1174][9496]. Th[1175]e[1176] d[1177]e[1178]
s[1179]c[1180]r[1181]i[1182]b[1183]e[1184]e[1185] h[1186]e[1187] e[1188]d[1189] t[1190]
h[1191]e[1192] d[1193]e[1194]r[1195]i[1196]f[1197]i[1198]e[1199]d[1200] e[1201]q[1202]u[1203]
i[1204]p[1205]e[1206]n[1207]t[1208] h[1209]a[1210]d[1211] a[1212]n[1213]i[1214]f[1215]
i[1216]c[1217]e[1218]n[1219] d[1220]i[1221]a[1222]d[1223] a[1224]s[1225]e[1226]d[1227]
d[1228]i[1229]p[1230]h[1231]e[1232]n[1233]e[1234]s[1235] i[1236]n[1237] e[1238]a[1239]
k[1240]f[1241]i[1242]e[1243]l[1244] ad[1245] p[1246] N[1247]e[1248]i[1249]n[1250]

On[1251] t[1252]h[1253] d[1254]e[1255]p[1256]t[1257]e[1258]m[1259]e[1260]n[1261]t[1262]
p[1263]e[1264]c[1265]t[1266]i[1267]f[1268]i[1269]c[1270] a[1271]c[1272]h

has been proposed in [97] and [98] and is called the Schwarzschild metric. A flat spacetime has been proposed in [99] and [100] and is called the Minkowski metric. The Schwarzschild metric is a solution of the Einstein field equations. The Minkowski metric is a solution of the Einstein field equations. The Schwarzschild metric is a solution of the Einstein field equations. The Minkowski metric is a solution of the Einstein field equations.

The Schwarzschild metric is a solution of the Einstein field equations. The Minkowski metric is a solution of the Einstein field equations. The Schwarzschild metric is a solution of the Einstein field equations. The Minkowski metric is a solution of the Einstein field equations. The Schwarzschild metric is a solution of the Einstein field equations. The Minkowski metric is a solution of the Einstein field equations. The Schwarzschild metric is a solution of the Einstein field equations. The Minkowski metric is a solution of the Einstein field equations.

The Schwarzschild metric is a solution of the Einstein field equations. The Minkowski metric is a solution of the Einstein field equations. The Schwarzschild metric is a solution of the Einstein field equations. The Minkowski metric is a solution of the Einstein field equations. The Schwarzschild metric is a solution of the Einstein field equations. The Minkowski metric is a solution of the Einstein field equations. The Schwarzschild metric is a solution of the Einstein field equations. The Minkowski metric is a solution of the Einstein field equations.

2 General panorama

The Schwarzschild metric is a solution of the Einstein field equations. The Minkowski metric is a solution of the Einstein field equations. The Schwarzschild metric is a solution of the Einstein field equations. The Minkowski metric is a solution of the Einstein field equations.

$$ds_{(g)}^2 = -\frac{(1 - \frac{2M}{r})}{\sqrt{(1 + \frac{3X}{4})(1 - \frac{X}{4})}} dt^2 + \frac{dr^2}{(1 - \frac{2M}{r})} \sqrt{\frac{(1 + \frac{3X}{4})}{(1 - \frac{X}{4})^3}} + r^2 (d\theta^2 + \sin^2 \theta d\phi^2), \quad (2.1)$$

where $X = \xi b^2$ is a constant, ξ is a constant, b is a constant, ξ is a constant, b is a constant.

The Schwarzschild metric is a solution of the Einstein field equations. The Minkowski metric is a solution of the Einstein field equations.

Hawking and [100] and ac-

cept [103]. It is a solution of the Einstein field equations.

in the end:

$$\lim_{r \rightarrow \infty} g_{tt} = \frac{1}{\sqrt{(1 + \frac{3X}{4})(1 - \frac{X}{4})}}. \text{ Given } X \text{ is a constant, } g_{tt} \text{ is a constant.}$$

the case

$$t \text{ as } [(1 + \frac{3X}{4})(1 - \frac{X}{4})]^{-1/4} t \rightarrow \tilde{t}, \text{ we } \tilde{t} \text{ is defined}$$

by the following definition:

$$f(r) \equiv 1 - \frac{2M}{r},$$

$$\alpha \equiv \frac{1}{\sqrt{(1 + \frac{3X}{4})(1 - \frac{X}{4})}}, \beta \equiv \sqrt{\frac{(1 + \frac{3X}{4})}{(1 - \frac{X}{4})^3}}. \text{ In this case, } \alpha \text{ and } \beta \text{ are constants.}$$

$$d\tilde{s}^2 = -f(r)d\tilde{t}^2 + \frac{\beta}{f(r)} dr^2 + r^2 (d\theta^2 + \sin^2 \theta d\phi^2). \quad (2.2)$$

2.1 Kretschmann scalar

The Kretschmann scalar is a scalar invariant of the Riemann curvature tensor. It is a solution of the Einstein field equations. The Kretschmann scalar is a scalar invariant of the Riemann curvature tensor. It is a solution of the Einstein field equations.

$$K = R_{\mu\nu\gamma\lambda} R^{\mu\nu\gamma\lambda}. \quad (2.3)$$

Here, $R_{\mu\nu\gamma\lambda}$ is Riemann tensor

$$K = \frac{4(12M^2 + 4(\beta - 1)Mr + (\beta - 1)^2r^2)}{\beta^2r^6}. \quad (2.4)$$

By setting $X = 0$ ($\beta = 1$), the Schwarzschild

$$\frac{48M^2}{r^6},$$

is recovered. For $\beta > 1$, the metric is a

deformation of the Schwarzschild

metric. The depth of the

potential well is shown in Fig. 1. The

potential well is shown in Fig. 1. The

$$r = -\frac{2M}{(\beta-1)}(1 \pm i\sqrt{2}) =$$

complex roots of the equation $K = 0$. The

potential well is shown in Fig. 1. The

potential well

$$r = 0$$

potential well is shown in Fig. 1. The

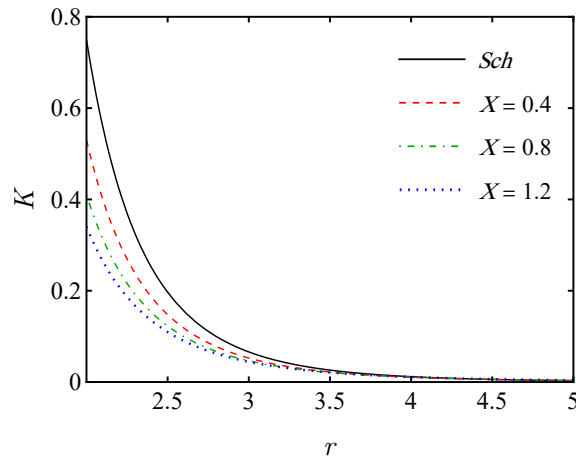


Fig. 1: The potential well

for $M = 1$

and $\beta = 1.2$

3 partial wave equation

The partial wave equation is

obtained from Eq. (2.2) as

$$\frac{1}{\sqrt{-g}}\partial_\mu(\sqrt{-g}g^{\mu\nu}\partial_\nu\Psi) = 0, \quad (3.1)$$

and the separation of variables

$$\Psi_{\omega lm}(\mathbf{r}, t) = \frac{\psi_{\omega l}(r)}{r} Y_{lm}(\theta, \varphi) e^{-i\omega t}. \quad (3.2)$$

In general, the metric can be

$$ds^2 = -g_{tt}dt^2 + g_{rr}dr^2 + r^2d\Omega^2,$$

where Ω^2 is the angular part.

$$dr^* = \frac{dr}{\sqrt{|g_{tt}g_{rr}^{-1}|}} = \sqrt{\beta} \frac{dr}{f(r)}, \quad (3.3)$$

where r^* is the tortoise coordinate.

The wave equation

$$\left[\frac{d^2}{dr^{*2}} + (\omega^2 - V_{eff}) \right] \psi_{\omega l}(r) = 0, \quad (3.4)$$

the effective potential V_{eff} is defined as

$$\begin{aligned}
 V_{eff} &= |g_{tt}| \left[\frac{l(l+1)}{r^2} + \frac{1}{r\sqrt{|g_{tt}g_{rr}|}} \frac{d}{dr} \sqrt{|g_{tt}g_{rr}^{-1}|} \right] \\
 &= f(r) \left[\frac{l(l+1)}{r^2} + \sqrt{\frac{(1-\frac{X}{4})^3}{(1+\frac{3X}{4})}} \frac{1}{r} \frac{df(r)}{dr} \right].
 \end{aligned}
 \tag{3.5}$$

From Fig 2, it is clear that V_{eff} decreases as X increases. For $X=0$, the potential is the same as the Schwarzschild case. As X increases, the potential barrier decreases.

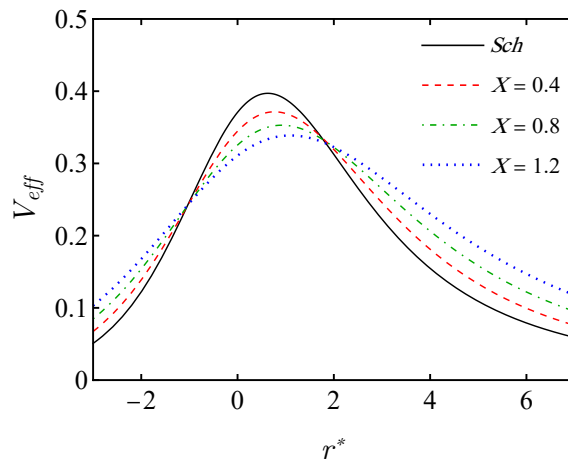


Fig 2: The effective potential V_{eff} versus r^* for $M = 0.5$, $l = 1$ and different values of X .

4 Absorption cross section

As shown in Fig 2, the scattering potential is real and finite. In this case, the scattering is elastic and the total flux is conserved. The scattering process can be described as follows [104, 105]

$$\psi_{\omega l} \approx \begin{cases} \mathcal{T}_{\omega l} R_1, & \text{for } r^* \rightarrow +r_h \text{ (} r \rightarrow -\infty \text{)} \\ R_2 + \mathcal{R}_{\omega l} R_2, & \text{for } r^* \rightarrow +\infty \text{ (} r \rightarrow \infty \text{)} \end{cases}
 \tag{4.1}$$

where $|\mathcal{R}_l|^2$ and $|\mathcal{T}_l|^2$ are the reflection and transmission coefficients respectively. Due to flux conservation, $|\mathcal{R}_l|^2 + |\mathcal{T}_l|^2 = 1$ is satisfied. Moreover, R_1 and R_2 can be written as [106]

$$R_1 = e^{-i\omega r^*} \sum_{j=0}^N (r - r_h)^j A_{r_h}^{(j)},
 \tag{4.2}$$

$$R_2 = e^{-i\omega r^*} \sum_{j=0}^N \frac{A_{\infty}^{(j)}}{r^j}.
 \tag{4.3}$$

To find the coefficients $A_\infty^{(j)}$ and $A_{r_h}^{(j)}$, we use the asymptotic expansion of the metric tensor $g_{\mu\nu}$ at large r and at the horizon $r=r_h$. The metric tensor is given by Eq. (3.4) and the Ricci scalar R is given by Eq. (3.5). The coefficients $A_\infty^{(j)}$ and $A_{r_h}^{(j)}$ are defined as [107]

$$e^{2i\delta_{\omega l}} = (-1)^{l+1} \mathcal{R}_{\omega l}. \quad (4.4)$$

To obtain the scattering cross-section, we use Eq. (4.2) and Eq. (4.3) and expand to 10th order ($N=10$). Since for $r \sim 200r_h$, we can use the asymptotic expansion of the metric tensor $g_{\mu\nu}$ at large r (Eq. (3.4)).

On the other hand, the scattering cross-section is given by [108]

$$\sigma_{abs} = \sum_{l=0}^{\infty} \sigma_{abs}^l, \quad \sigma_l \text{ is}$$

$$\sigma_{abs}^l = \frac{\pi}{\omega^2} (2l+1) (1 - |e^{2i\delta_{\omega l}}|^2). \quad (4.5)$$

By Eq. (4.4) and the definition of the phase $\delta_{\omega l}$ [109], we can write the phase $\delta_{\omega l}$ as

$$|e^{2i\delta_{\omega l}}|^2 = 1 - |\mathcal{R}_{\omega l}|^2 = |T_{\omega l}|^2 \propto e^{-i\omega\sqrt{\beta}r}.$$

β and r are

$$\sigma_{abs} = \frac{\pi}{\beta\omega^2} \sum_{l=0}^{\infty} (2l+1) |T_{\omega l}|^2, \quad (4.6)$$

where $|T_{\omega l}|^2$ is the transmission coefficient. The scattering cross-section σ_{abs} can be calculated by using Eq. (4.6).

Fig. 3 shows the scattering cross-section $\sigma_{abs}/4\pi M^2$ as a function of $2M\omega$ for $l=0, 1, 2$ and different values of X ($X=0, 0.4, 0.8, 1.2$). The scattering cross-section decreases as l increases and as X increases. The scattering cross-section is shown in Fig. 4 for $l=0$ and $l=1$ for different values of X .

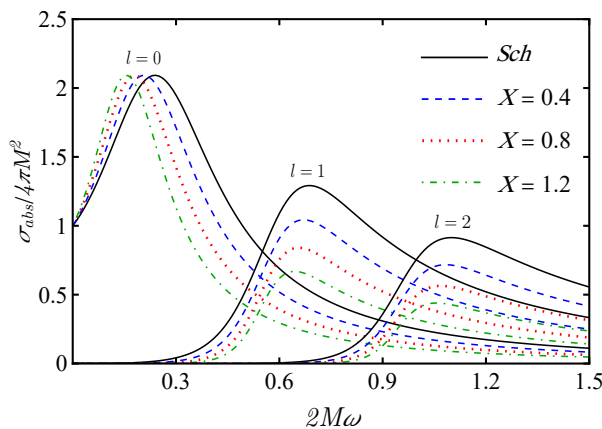


Fig. 3: Scattering cross-section $\sigma_{abs}/4\pi M^2$ as a function of $2M\omega$ for $l=0, 1, 2$ and different values of X .

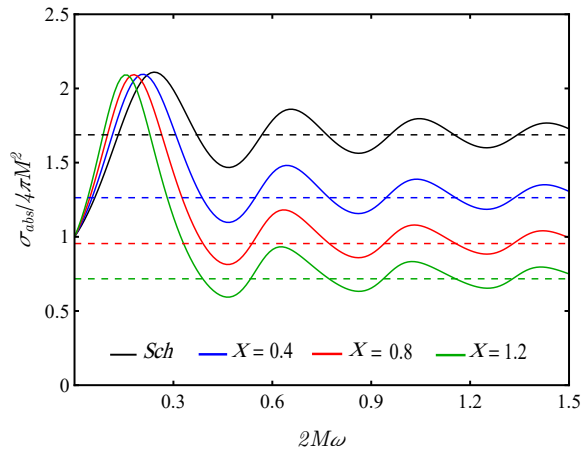


Fig 4: Total cross-section $l = 6$ for different values of X . The curves are plotted by taking $b_c = 1.5$.

4.0.1 High frequency regime

The high frequency regime is characterized by $\beta \gg 1$. In this regime, the cross-section σ_{geo} is dominated by the geometric cross-section σ_{GR} , which is given by

$$\sigma_{geo} = \frac{\pi b_c^2}{\beta}, \quad (4.7)$$

where b_c is the critical impact parameter. The critical impact parameter b_c is determined by the condition $-f(r)t^2 + f(r)^{-1}\beta\dot{r}^2 + r^2\dot{\phi}^2 = 0$. By using the energy E and angular momentum L , we can write the condition as

$$\beta r^2 + \tilde{V}_{eff} = 0, \quad (4.8)$$

where \tilde{V}_{eff} is defined by

$$\tilde{V}_{eff} = E^2 - \frac{f(r)}{r^2} L^2. \quad (4.9)$$

The critical impact parameter $r = r_c$ is determined by the condition

$$\tilde{V}_{eff} = 0, \quad (4.10)$$

$$\frac{d\tilde{V}_{eff}}{dr} = 0. \quad (4.11)$$

Each equation is satisfied by

$$2f(r_c) - r_c f'(r_c) = 0, \quad (4.12)$$

$$b_c = \frac{r_c^2}{f(r_c)}, \quad (4.13)$$

where we have defined $b = L/E$. We can see that b_c is a function of r_c and $f(r_c)$. The critical impact parameter b_c is determined by the condition $3M < b_c < 3\sqrt{3}M$, which is satisfied by Eq(4.7), where

$$\sigma_{geo} = \sigma_{GR}/\beta.$$

In Fig 4, a plot of absorption coefficient σ_{geo} versus X . According to the plot, the absorption coefficient σ_{geo} increases with X . It is also observed that the absorption coefficient σ_{geo} is independent of ω .

$$l = 6$$

5 Greybody Factor

The absorption coefficient is related to the Hawking radiation. The Hawking radiation is described by the WKB method in Ref [101]. The absorption coefficient σ_{geo} is given by [110-112]. In this paper, we calculate the absorption coefficient σ_{geo} by

$$T_b \geq \text{sech}^2 \left(\int_{-\infty}^{+\infty} \mathcal{G} dr^* \right), \quad (5.1)$$

$$\mathcal{G} = \frac{\sqrt{(h')^2 + (\omega^2 - V_{eff} - h^2)^2}}{2h}. \quad (5.2)$$

Here h is a function of r and ω . $h(r^*) > 1$ and $h(-\infty) = h(+\infty) = \omega$. Substituting $h(r)$ in Eq (3.5) we get

$$T_b \geq \text{sech} \left(\frac{1}{2\omega} \left(l(l+1) + \frac{\sqrt{(1 - \frac{X}{4})^3}}{2\sqrt{1 + \frac{3X}{4}}} \right) \right)^2. \quad (5.3)$$

Fig 5: The plot of the absorption coefficient T_b versus ω for different values of X .

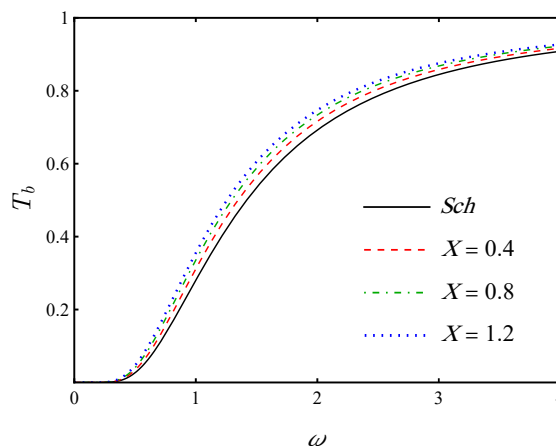


Fig 5: The plot of the absorption coefficient T_b versus ω for different values of X .

The absorption coefficient T_b is reflected as the Hawking radiation. The absorption coefficient T_b is independent of ω . When the frequency ω is small, the absorption coefficient T_b is zero. As ω increases, the absorption coefficient T_b increases and approaches 1.

decrease the growth rate of the perturbation. In the case of Schwarzschild black holes, the growth rate decreases linearly with the horizon radius.

X. The6, an $X \neq 0$,
X increases polynomially

6 Quasinormal modes

6.1 The scaling of spherical modes and long-living modes

On the one hand, the quasinormal modes (QNMs) of black holes (BHs) and neutron stars (NSs) are studied in [113], and extended to rotating BHs in [114]. In the case of a rotating BH, the QNMs are complex, and the real part represents the frequency and the imaginary part represents the damping rate.

We start with the spherically symmetric case, where the QNM equation is

$$\psi(r) = \left(\frac{r}{2M} - 1\right)^\rho \left(\frac{r}{2M}\right)^{-2\rho} \exp[-\rho(r/2M - 1)] \sum_{n=0}^N a_n \left(\frac{r - 2M}{r}\right)^n, \quad (6.1)$$

with $\rho = -i\sqrt{\beta}\omega$. By substituting this ansatz into the QNM equation, we obtain

$$\alpha_n a_{n+1} + \beta_n a_n + \gamma_n a_{n-1} = 0, \quad \text{with } n \geq 1, \quad (6.2)$$

$$\alpha_0 a_1 + \beta_0 a_0 = 0, \quad (6.3)$$

where

$$\alpha_n = (n+1) \left(-4i\sqrt{\beta}M\omega + n + 1\right), \quad (6.4)$$

$$\sigma_n = 32\beta M^2 \omega^2 + 8i\sqrt{\beta}M\omega + 16i\sqrt{\beta}Mn\omega - 2n(n+1) - \beta l(l+1) - 1, \quad (6.5)$$

$$\gamma_n = \left(n - 4i\sqrt{\beta}M\omega\right)^2. \quad (6.6)$$

We can also write the QNM equation as

$$\frac{\sigma_0}{\alpha_0} - \frac{\gamma_1}{\sigma_1 - \frac{\alpha_1 \gamma_2}{\sigma_2 - \frac{\alpha_2 \gamma_3}{\sigma_3 - \dots}}} = 0, \quad (6.7)$$

where ω is the QNM frequency. In the case of a rotating BH, the QNM equation is more complicated, and the growth rate is not purely imaginary.

ω is the QNM frequency. N is the truncation order. X .

Using the asymptotic expansion of the QNM equation, we can obtain the scaling of the QNM frequencies in the limit of large N .

$$\delta = \frac{\omega_{R,I}}{\omega_{R,I|GR}} - 1, \quad (6.8)$$

where $\omega_{R,I|GR}$ is the real and imaginary parts of the QNM frequency in the Schwarzschild case. We also define

Before the end of the Schwarzschild case, we also define $l = 0$ case can be computed analytically, in the GR case. For the spherically symmetric case, $l = 0$ is valid for

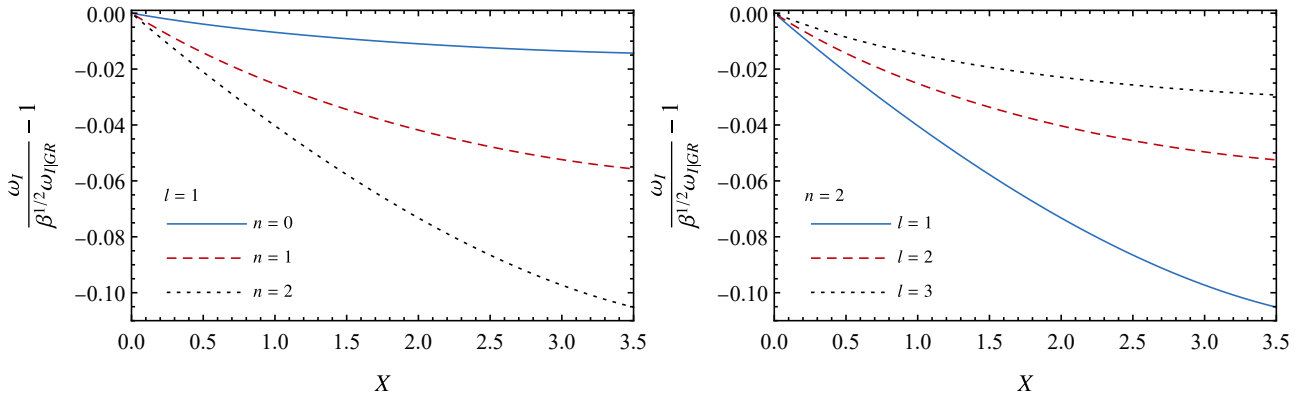


Fig 6: Real part of the dimensionless frequency $\frac{\omega_I}{\beta^{1/2}\omega_{I|GR}} - 1$ versus X , for $l = 1, 2, 3$ and $n = 0, 1, 2$. The curves are in color (blue) and for l (red).

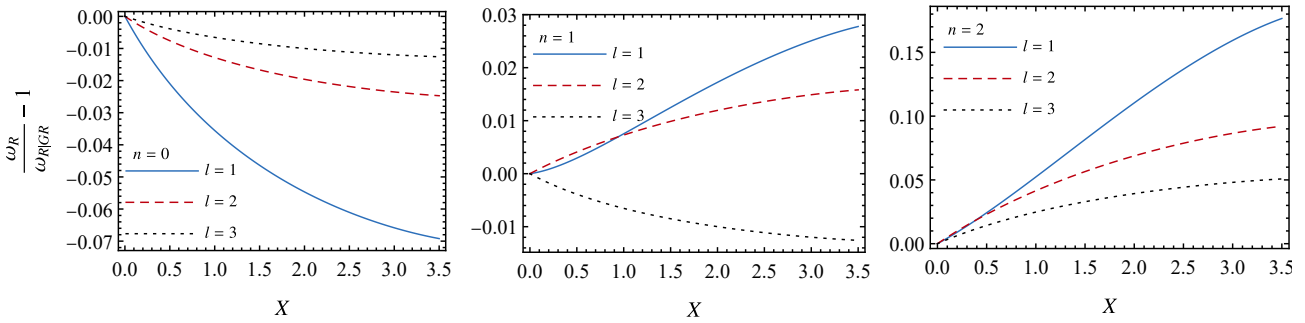


Fig 7: Imaginary part of the dimensionless frequency $\frac{\omega_R}{\omega_{R|GR}} - 1$ versus X .

In the GR case, the real part of the frequency is given by

$$\omega = \beta^{-1/2}\omega_{GR} \quad (l = 0). \quad (6.9)$$

Thus, as $\beta \rightarrow \infty$ ($X \rightarrow 4$), the real part of the frequency approaches the GR value. We have checked this numerically by comparing the results with the GR case.

For $l > 0$, the real part of the frequency is given by the solution of the characteristic equation (6.7), which is independent of the parameters n and l .

$$\omega_I \approx \beta^{-1/2}\omega_{I|GR}. \quad (6.10)$$

In Fig 6, we show the real part of the dimensionless frequency (6.10) for $l = 0, 1, 2$, and $n = 0, 1, 2$. We see that the curves are nearly identical for l and n . In case of Fig 6, we observe that the real part of the frequency is approximately 10% smaller than the GR value as $\beta \rightarrow \infty$ ($X \rightarrow 4$). From Fig 7, we observe that the imaginary part of the dimensionless frequency is approximately 10% smaller than the GR value as $\beta \rightarrow \infty$ ($X \rightarrow 4$). In Fig 7, we observe that the imaginary part of the dimensionless frequency is approximately 10% smaller than the GR value as $\beta \rightarrow \infty$ ($X \rightarrow 4$). We observe that for $n = 0, 1, 2$ and $l = 1, 2, 3$, the curves are nearly identical for n and l .

6.2 Relation between Shadow radius and quasinormal mode

As discussed in Sec. 4.1, the shadow radius is characterized by the

equation $\omega_R - i\omega_I = 0$. In this section, we study the QNMs of the black hole and the Lyapunov exponent λ [115]

$\omega =$

$$\omega = l\Omega - i(n + \frac{1}{2})|\lambda|. \quad (6.11)$$

where Ω and λ denote the Lyapunov exponent, respectively. The Lyapunov exponent λ is also related to the

shadow radius R_{sh} [116–118]. The Lyapunov exponent

is related to the shadow radius R_{sh} [119–121] and the Lyapunov exponent

is

$$\omega_R = \lim_{l \gg 1} \frac{l}{R_{sh}}. \quad (6.12)$$

The Lyapunov exponent λ is related to the Lyapunov exponent

at the Lyapunov exponent λ [122], Eq. (6.12) is

$l \gg 1$ ad, ref [122], Eq. (6.12) is

related to the Lyapunov exponent as

$$\omega_R = \lim_{l \gg 1} \frac{l + \frac{1}{2}}{R_{sh}}. \quad (6.13)$$

The Lyapunov exponent λ is related to the Lyapunov exponent

at the Lyapunov exponent λ [120, 123]. Fig. 124, the Lyapunov

exponent λ is related to the Lyapunov exponent λ by

$r_c = 3M$. Now by

$$R_{sh} = \sqrt{\frac{r_c^2}{f(r_c)}}, \quad (6.14)$$

the Lyapunov exponent λ is related to the Lyapunov exponent

at the Lyapunov exponent λ [120, 123]. In Fig. 8, the Lyapunov

exponent λ is related to the Lyapunov exponent λ by

$$l + \frac{1}{2} \text{ and } \lambda \text{ is related to } \omega_R$$

$1 < l < 120$.

The Lyapunov exponent λ is related to the Lyapunov exponent

at the Lyapunov exponent λ [120, 123]. The Lyapunov

exponent λ is related to the Lyapunov exponent λ by

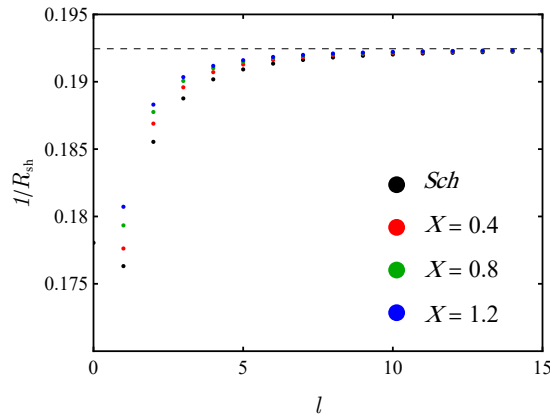


Fig. 8: The Lyapunov exponent

$\omega_R (l + \frac{1}{2})^{-1}$ and the Lyapunov exponent λ is related to

the Lyapunov exponent λ [120, 123]. The Lyapunov

exponent λ is related to the Lyapunov exponent λ by

7 Emission rate

The black hole emission rate is calculated as
 in the case of a Schwarzschild black hole
 by the Hawking radiation process
 and is given by [125, 126] as

$$\frac{d^2 E}{d\omega dt} = \frac{2\pi^2 \sigma_{lim}}{e^{\frac{\omega}{T_H}} - 1} \omega^3, \tag{7.1}$$

where ω is the frequency, T_H is the Hawking temperature. The
 emission rate is $\sigma_{lim} \approx \pi R_h^2$. Substituting
 Eq. 6.14 and the Hawking temperature, we get

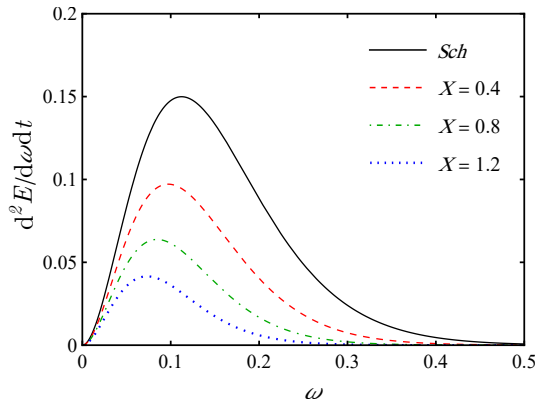


Fig 9: The behavior of the emission rate for $M = 1$.

In Fig 9, the emission rate is plotted for
 different values of X . It can be seen that
 the emission rate decreases as X increases.

8 Conclusion

In this work, we have studied the emission rate
 of a Schwarzschild black hole. We have
 shown that the emission rate is given by
 $r = 0$. We

We can see from the above plot that
 the emission rate decreases as X increases.
 This is because the Hawking temperature
 decreases as X increases.

By using the above results, we can
 calculate the emission rate for different
 values of X .

bntbee backshash pthijngdes wgrn
 dngalseno
 Thryegh ellhwed hth copene beverh ealpt6
 QNMsad h hndisabafied indfied gthom Faly h
 anyth engine, who discod hth bntbee or afia pater
 hsa dngcth eme, dengha hgrbntbee paterlv
 etia brcappesth back hthfow

References

- [1] Siddesad MatVer Cawthitblscalahy *Phys. Rev. D*, 68:045001, 2003.
- [2] H. P. Rben Pbe esvstith scalyhfy *Rev. Mod. Phys.*, 21:378382, 1949.
- [3] RberC. Mysad MainPob Uhtdficafidpichin *Phys. Rev. Lett.*, 90:211601, 2003.
- [4] O. Behind J. G. Ra. Bdsrbic bntgish findpr *Phys. Rev. D*, 71:097901, 2005.
- [5] C. M. Reys L. F. Un, ad J. D. Vega. Quantth asptiel *Phys. Rev. D*, 78:125011, 2008.
- [6] Daid MagHaw wted bntine eg *arXiv preprint arXiv:0802.1561*, 2008.
- [7] G.I. Rbbs P.S. San ad S.M. Sbjn Th flene fbntb *CPT and Lorentz Symmetry*, pg 192495, 2014.
- [8] Sead Lbeat Testbrinne: a 2013 dae. *Classical and Quantum Gravity*, 30(13):133001, 2013.
- [9] JayD Tas Whtdowabntinne? *Reports on Progress in Physics*, 77(6):062901, 2014.
- [10] An éenHees QuhG Baly AdenBg PhnLe Bas Ch Gah *Universe*, 2(4):30, 2016.
- [11] CaRol *Quantum gravity. Cahile ups* 2004.
- [12] V. AhrKseck yad SurSani Spobreakfbrnyg *Phys. Rev. D*, 39:683685, 1989.
- [13] V. AhrKseck yad SurSani Phobalgnlcnng *Phys. Rev. Lett.*, 63:224227, 1989.
- [14] V. AhrKseck yad SurSani Gavnlpnhrdenil *Phys. Rev. D*, 40:18864903, 1989.
- [15] V. AhrKseck yad RbesPg Cpad g *Nuclear Physics B*, 359(2):545 – 570, 1991.

- [16] V. AnKock yad RbesPg Cp g ad anicbs *Phys. Rev. D*, 51:39233935, 1995.
- [17] RdGabiad Jg Ph Ndad psfapce-in *Phys. Rev. D*, 59:124021, 1999.
- [18] MahBjil, HgA. MlesT ecþ ad HanSahm Lpny *Phys. Rev. D*, 71:084012, 2005.
- [19] GinAonCach ad ShhMajl. Wæsnob pccenad gmaybs *International Journal of Modern Physics A*, 15(27):43014323, 2000.
- [20] SeanM. Cab JefyA. Hary V. AnKock ý ChsD. Laa, ad Takin *Phys. Rev. Lett.*, 87:141601, 2001.
- [21] LeadoMdes Sprentbe QutGaj *Phys. Rev. D*, 86:044005, 2012.
- [22] J. R. Nasin A. YuPead P. J. P6 ío CaslG delþ acsiral *Eur. Phys. J. C*, 81(9):815, 2021.
- [23] FasR. Kherad ChRp Spacemncpnyad pg- in *Phys. Rev. D*, 70:045020, 2004.
- [24] S. Bend ad F. R. Kher Bdsbsaesfchisalpcemfm *Phys. Rev. D*, 75:024028, 2007.
- [25] F.R. Kher Z-þalgg anjad brinne. *Nuclear Physics B*, 535(1):233 –241, 1998.
- [26] F.R. Kher A cpny *Nuclear Physics B*, 578(1):277 –289, 2000.
- [27] F.R. Kherad J. Schi Cpny a gñilic *Nuclear Physics B*, 639(1):241 –262, 2002.
- [28] K.J.B. Glad F.R. Kher Anbnad cpñfa bal chsk erih efcc gg-fiedl ach *Nuclear Physics B*, 926:335 –369, 2018.
- [29] PetHo ña. Qutñata ð *Phys. Rev. D*, 79:084008, 2009.
- [30] GüCb, RabayMyl LonSebanSnWagad SeZebn Cnth ña-k ad ic hekny çalad pha- b *Classical and quantum gravity*, 33(22):225014, 2016.
- [31] AesdcashMahRadj LonSebaninad SyVag At ad ol ic gñad a gñeresñty *Classical and Quantum Gravity*, 36(1):017001, 2018.
- [32] V AnKock yad NelRal Daa abesfmad c pñb *Reviews of Modern Physics*, 83(1):11, 2011.
- [33] DnChdayad PaçkMcDad. Saçalachnsad bñb *Physical Review D*, 70(12):125007, 2004.
- [34] A. A An jFh Lonñisñia haleso *The European Physical Journal Plus*, 136(4):144, 2021.

- [35] A. A. A. and R. V. M. *Brazilian Journal of Physics*, 51(3):820830, 2021.
- [36] M. A. A. and E. M. *Physics Letters B*, 785:191496, 2018.
- [37] R. C. and M. F. Jr. *Physical Review D*, 78(12):125013, 2008.
- [38] R. C. and M. F. Jr. *Physical Review D*, 80(8):085026, 2009.
- [39] A. A. A. and A. Y. *The European Physical Journal C*, 81(9):843, 2021.
- [40] A. R. and G. F. *The European Physical Journal C*, 81(5):459, 2021.
- [41] T. M. J. R. N. and A. Y. *Phys. Rev. D*, 85:125003, 2012.
- [42] J. A. A. S. *The European Physical Journal Plus*, 136(3):310, 2021.
- [43] A. A. A. and A. Y. *International Journal of Modern Physics A*, 36(34 & 35):2150242, 2021.
- [44] J. F. and H. H. *arXiv preprint arXiv:2305.08587*, 2023.
- [45] A. A. A. *arXiv preprint arXiv:2201.00066*, 2021.
- [46] S. M. C. and G. B. *Physical Review D*, 41(4):1231, 1990.
- [47] S. M. C. and H. T. *Physical Review D*, 78(4):044047, 2008.
- [48] M. G. J. R. N. and A. Y. *Phys. Rev. D*, 81:045018, 2010.
- [49] D. C. and V. A. *Physical Review D*, 58(11):116002, 1998.
- [50] V. A. *Physical Review D*, 69(10):105009, 2004.
- [51] V. A. *Physical Review D*, 103(2):024059, 2021.
- [52] R. B. H. and V. A. *Physical Review D*, 68(12):125008, 2003.

- [53] Robert H. Brand and V. Alan Kock, *Spontaneous symmetry breaking and gravity*, *Physical Review D—Particles, Fields, Gravitation, and Cosmology*, 71(6):065008, 2005.
- [54] Robert H. Brand and V. Alan Kock, *Spontaneous symmetry breaking and gravity*, *Physical Review D—Particles, Fields, Gravitation, and Cosmology*, 77(6):065020, 2008.
- [55] Robert Brand and Yu. Yagajko, *Spontaneous symmetry breaking*, *Symmetry*, 13(4):660, 2021.
- [56] Robert Brand and Yu. Zh. Spasov, *Spontaneous symmetry breaking in curved spacetime fields*, *Symmetry*, 16(1):25, 2023.
- [57] V. Alan Kock and Jay D. Tan, *Materialized branes*, *Physical Review D—Particles, Fields, Gravitation, and Cosmology*, 83(1):016013, 2011.
- [58] O. Behar and J. Pantoja, *Vacuum field electrodynamics*, *Physical Review D*, 72(4):044001, 2005.
- [59] R. Casati, A. Cattaneo, F. P. ad E. B. S. Exact solutions, *Physical Review D*, 97(10):104001, 2018.
- [60] A. F. S. WDR, J. R. Nasir, and A. Yu. P. G., *deliberate behavior*, *Modern Physics Letters A*, 30(02):1550011, 2015.
- [61] WDR, J. S. ad A. F. S. G., *deliberate behavior*, *International Journal of Modern Physics A*, 35(09):2050050, 2020.
- [62] WDR, J. S. ad A. F. S. R. C. id. a. k. e. n. g. i. n. e. e. r. g. i. d. e. l., *Modern Physics Letters A*, 34(22):1950171, 2019.
- [63] R. V. M. ad J. R. C. S. N. e. e. s. B. a. c. k. s. t. a. c. a. l. c. o. n. t. r. i. b. u. t. i. o. n. e. e. s., *Physical Review D*, 103(4):044002, 2021.
- [64] R. V. M. ad J. R. C. S. N. e. e. s. B. a. c. k. s. t. a. c. a. l. c. o. n. t. r. i. b. u. t. i. o. n. e. e. s., *Physical Review D*, 103(4):044002, 2021.
- [65] S. R. K. ad H. B. ad A. R. ad B. B. e. e. e. g. i. a. d. p. e. t. e. r. i. e. r. o. n. e. p. e. r. i. o. d. s., *Journal of Cosmology and Astroparticle Physics*, 2021(04):036, 2021.
- [66] R. X. ad D. C. ad L. S. ad S. S. a. t. p. r. a. c. t. i. v. i. t. y. b. e. h. a. v. i. o. r., *Physical Review D*, 107(2):024011, 2023.
- [67] R. V. M. ad J. R. C. S. N. e. e. s. B. e. h. a. v. i. o. r. f. i. e. l. d. a. s. a. n. d. f. o. r. g. a. l. a. p. s., *JCAP*, 10:038, 2021.
- [68] S. R. K. ad H. B. ad A. R. ad B. B. e. e. e. g. i. a. d. p. e. t. e. r. i. e. r. o. n. e. p. e. r. i. o. d. s., *JCAP*, 04:036, 2021.
- [69] Ted Jacobson and David Matyjewicz, *Spontaneous symmetry breaking*, *Physical Review D*, 64(2):024028, 2001.
- [70] R. Jackiw and S.-Y. Pi, *Chiral fermions*, *Physical Review D*, 68(10):104012, 2003.

- [88] Benjamin Edwards V. Ankeck Renfrew and Leon
bisarfields *Phys. Lett. B*, 786:319326, 2018.
- [89] M. Schck Chisallansad Frustusin Lonbi
fin *Eur. Phys. J. C*, 75(5):187, 2015.
- [90] DChdayad PakMcDad. ShLonVhLaggsad Asaed
FrStas *Phys. Rev. D*, 92(8):085031, 2015.
- [91] M. Schck Chisallaggsad Frustusin infisco
th Sadad-MdelEsa *Phys. Rev. D*, 93(10):105017, 2016.
- [92] D. M. Ghoea. Pahnat gy pasbeaggsad sae gy
ad flah *Eur. Phys. J. C*, 80(12):1147, 4 2020.
- [93] D. M. Ghoea. Gagsae gpad flah WeyesPahingy *Eur.
Phys. J. C*, 81(6):510, 2021.
- [94] Adn DehJ. R. Nasim GabJ. OhA. YuPeaad PabJ. P6 *io
Met-afin bhebee gy chisalapcs* *Eur. Phys. J. C*, 81(4):287, 2021.
- [95] Adr à DehJ. R. Nasim GabJ. OhA. YuPeaad PabJ. P6 *io
Radiac cocicac-afin bhebee del* *Phys. Lett. B*, 826:136932, 2022.
- [96] Adr à DehT. Maiz J. R. Nasim GabJ. OhA. YuPeaad PabJ.
P6 *io SpadLonpbeaggsad a-jecc acicb ac-
afin bhebee gy* *JCAP*, 07(07):018, 2022.
- [97] A. A. An jFhJ. R. NasimA. YuPeaad P. J. P6 *io Vacuu
a ac-afin bhebee gy* *Phys. Rev. D*, 108(8):085010, 2023.
- [98] A. A. An jFhJ. R. NasimA. YuPeaad P. J. P6 *io Areactahax
ic acicbu acafin bhebee gy* *Journal of Cosmology
and Astroparticle Physics*, 2024(07):004, 2024.
- [99] GaetanLabis, LendoMabop Reg C. Paig ad Al Og Pbig
sheli-k backbsic-afin bhebee gyluccehuk
ng, gydybds ad npegh *JCAP*, 12:026, 2023.
- [100] ShKunJh ad AsRahan Styfoides gydybds ad
pghadaita ac-afin bhebee gyluc *arXiv
preprint arXiv:2310.06492*, 2023.
- [101] A. A. An jFhH Hasanbadj N Heidar J Kr *iz ad S Zae. Gantlncesb
bhebee gyncafin fin* *Classical and Quantum Gravity*, 41(5):055003,
2024.
- [102] A. A. Aa jFhJ. R. NasimA. YPeaad P. J. P6 *io Gantleby
a bntbackh.* *arXiv preprint arXiv:2404.04176*, 2024.
- [103] GaetanLabis, LendoMabop Reg C Paig ad Al *Ög ü Pbig
sheli-k backbsic-afin bhebee gyluccehuk* *Journal of Cosmology and Astroparti-
cle Physics*, 2023(12):026, 2023.

- [104] CaiFB MacedoEdts de Oba, ad Lu isCB Cp Scatibylrbck
 bs pamsahrasw badeerback. *Physical Review D*,
 92(2):024012, 2015.
- [105] CaiFB MacedoLICS Lee, ad Lu isCB Cp Abbydibackhs Nli
 gdesad sahras *Physical Review D*, 93(2):024027, 2016.
- [106] CaiFB MacedoLICS Lee, Edts Oba, SarR Dbnad LICB Cp Ab-
 pamsahraswyrbackhs *Physical Review D*, 88(6):064033,
 2013.
- [107] SarR DbnEdts Oba, ad Lu isCB Cp Scatigd asbya
 canalack b. *Physical Review D*, 79(6):064014, 2009.
- [108] LuisCB CpSarR Dbnad Edts Oba. Scatimssahras
 byards ihackhs *Physical Review D*, 79(6):064022, 2009.
- [109] LICB CpAHighEdts Oba, ad Jg V Roh. Gedyfics
 fncpd sahrfiedsichde rpecm *Physical Review*
D, 87(10):104034, 2013.
- [110] MatVer Senanal bdsfo-dim saeg *Physical Review A*,
 59(1):427, 1999.
- [111] Peap Bond MatVer Bdiq bhwoficis *Annals of Physics*,
 323(11):27792798, 2008.
- [112] İztSaklad Saa Kan Tpaliewedyficsad qindesf
 bchshisefiphs *Turkish Journal of Physics*, 46(2):51–
 103, 2022.
- [113] Edard W Lear Anany epsnch qindesfkrback
 bs *Proceedings of the Royal Society of London. A. Mathematical and Physical Sciences*,
 402(1823):285298, 1985.
- [114] PabPan Adaned MelshBackHb PebanThy *Int. J. Mod. Phys. A*,
 28:1340018, 2013.
- [115] ViCadoAeXS Mada, Enme Bej HeiWekad Vif ZanhGedeis
 ably rpean ad qindes *Physical Review D*, 79(6):064016,
 2009.
- [116] IanZiSeinSphS Yazdjvad GalG Gghv Cactbeerback
 b qindesad ligh gdeflectm *Physical review letters*,
 104(25):251103, 2010.
- [117] ShoWenWei YuXadLi ad HegGo Reapbeengabp
 cscad qindiback. *Physical Review D*, 84(4):041501,
 2011.
- [118] ShoWenWei ad YuXadLi Eabh inalibetengilaws
 ad bckh eg *Physical Review D*, 89(4):047502, 2014.
- [119] Kauli. Cactbeerh hduind qindesingce-
 ts *Physical Review D*, 101(12):124063, 2020.

- [120] ChLi TaoZhQingWuKenJi, MbarJahMup AzgA inad
 AbWagShard qidcsa nqthack. *Phys-*
ical Review D, 101(8):084001, 2020.
- [121] KenJi. Quidcsa backsd bydakt rad hinc-
 ita hduia *Physical Review D*, 101(8):084055, 2020.
- [122] B CadMegr RDB Fan, ad Jéscde Ovi. Anyalcsene be-
 verduadad back qalfqies *Physics Letters B*, 811:135966,
 2020.
- [123] ShJé Ma, TarChMa, JarBoDeg ad XarRuHu Shdofshd back
 h in cl daktmb *Modern Physics Letters A*, 38(2425):2350104, 2023.
- [124] VerPetkad OegYuTp Caktback h adw Revvanyal
 des *Physics Reports*, 947:139, 2022.
- [125] YesD écanGtsEPFacs, ad Ab Focci Unifhngab-
 pscifhacks *Physical Review D*, 83(4):044032, 2011.
- [126] UnPapad FarAurRighd back h id esignt
 gy Pind idw *Physics of the Dark Universe*, 35:100916, 2022.